Latin American Journal of Solids and Structures
www.lajss.org

Semi-analytical Vibration Characteristics of Rotating Timoshenko Beams Made of Functionally Graded Materials

Abstract

Free vibration analysis of rotating functionally graded (FG) thick Timoshenko beams is presented. The material properties of FG beam vary along the thickness direction of the constituents according to power law model. Governing equations are derived through Hamilton's principle and they are solved applying differential transform method. The good agreement between the results of this article and those available in literature validated the presented approach. The emphasis is placed on investigating the effect of several beam parameters such as constituent volume fractions, slenderness ratios, rotational speed and hub radius on natural frequencies and mode shapes of the rotating thick FG beam.

Keywords

Free Vibration, Functionally Graded material, Rotating Beam, Differential Transform Method, power-law model.

Farzad Ebrahimi*
Mohadese Mokhtari

Department of Mechanical Engineering, Faculty of Engineering, Imam Khomeini International University, Qazvin, Iran, P.O.B. 16818-34149

*Corresponding Author email: febrahimy@eng.ikiu.ac.ir

http://dx.doi.org/10.1590/1679-78251446

Received 06.07.2014
In revised form 25.11.2014
Accepted 26.01.2015
Available online 07.02.2015

1 INTRODUCTION

The laminated composite structures can be tailored to design advanced structures, but the sharp change in the properties of each layer at the interface between two adjacent layers causes large interlaminar shear stresses that may eventually give rise to well-known phenomenon known as delamination. Such detrimental effects can be mitigated by grading the properties in a continuous manner across the thickness direction resulting in a new class of materials known as 'functionally graded materials' (FGMs) (Ebrahimi, 2013). In an effort to develop the super heat resistant materials, Japanese material scientists proposed the concept of FGM in the early 1980s. These materials, which are microscopically heterogeneous and are typically made from isotropic components, such as metals and ceramics, were initially designed as thermal barrier materials for aerospace structures and fusion reactors (Ebrahimi & Rastgoo, 2008a, b). FGMs are composite materials with inhomogeneous

micromechanical structure and are generally composed of two different parts such as ceramic and metal in which the material properties changes smoothly between two surfaces. This kind of material as a novel generation of composites of microscopical heterogeneity are achieved by controlling the volume fractions, microstructure, porosity, etc. of the material constituents during manufacturing, resulting in spatial gradient of macroscopic material properties of mechanical strength and thermal conductivity. As a result, In comparison with traditional composites, FGMs possess various advantages, for instance, ensuring smooth transition of stress distributions, minimization or elimination of stress concentration, and increased bonding strength along the interface of two dissimilar materials. Therefore, FGMs have received wide applications in modern industries including aerospace, mechanical, electronics, optics, chemical, biomedical, nuclear, and civil engineering to name a few during the past two decades. Motivated by these engineering applications, FGMs have also attracted intensive research interests, which were mainly focused on their static, dynamic and vibration characteristics (Ebrahimi et al. 2009a, b).

Further, the increasing use of beams as structural components in various fields such as marine, civil and aerospace engineering has necessitated the study of their vibration behavior and a large number of studies can be found in literature about transverse vibration of uniform isotropic beams. In this study, a relatively new approach called differential transformation method (DTM) is applied in analyzing vibration analysis of rotating FG beams. The concept of DTM was first proposed by Zhou (1986) in solving linear and non-linear initial value problems in electrical circuit analysis. The superiority of the DTM is its simplicity and good precision and depends on Taylor series expansion while it takes less time to solve polynomial series. It is different from the traditional high order Taylor's series method, which requires symbolic computation of the necessary derivatives of the data functions. With this method, it is possible to obtain highly accurate results or exact solutions for differential equations. With this technique, the given partial differential equation and related initial conditions are transformed into a recurrence equation that finally leads to the solution of a system of algebraic equations as coefficients of a power series solution. This method is useful for obtaining exact and approximate solutions for linear and nonlinear ordinary and partial differential equations and there is no need for linearization or perturbation. Also large computational work and round-off errors are avoided. It's a proper method to analyze beam vibrations. Study on rotating Timoshenko beams by differential transform method has been presented by some researchers (Ho and Chen, 2006; Mei, 2008).

In comparison with FGM shells and plates, there are fewer researches in literature about FGM beams. Among those, Navier type solution method has been applied by Aydogdu and Taskin (2007) to study free vibration of FG beams with simply supported edges. Kapuria et al. (2008) found vibration response of layered FG beams. Li et al. (2013) suggested a unified approach for analyzing free vibration of Euler and Timoshenko FG beams. Sina et al. (2009) analyzed the free vibration of FG beams with an analytical method; they used a new beam theory which is a little different from first-order shear deformation beam theory. Simsek (2010) has studied free vibration response of FG beam for different higher order beam theories. Recently Pradhan and Chakraverty (2013) have presented free vibration response of Euler and Timoshenko FG beams under various boundary conditions. Ke et al. (2010) have studied nonlinear vibration of non-rotating FG beams using both exponential law and power law distribution of material properties. Recently, Li et al (2013) has inves-

tigated the free vibration of non-rotating functionally graded beams with exponential variation of material properties. It is to be mentioned that in two above aforesaid articles the FG beam is not rotating.

Rotating beams play an important role in the modeling of engineering applications such as turbine blades, airplane propellers and robot manipulators among others. This subject has been investigated with different level of intensity, at least, over the last four decades. However, to the best of the author's knowledge, the research work on rotating beams made of functionally graded materials is scarce. Recently Mohanty et al. (2013) used finite element method to study free vibration of sandwich and ordinary rotating FG beams. Shahba et al. (2013) have investigated the free vibration of centrifugally stiffened tapered FG beams. However, in these formulations the material properties of beam vary along the length of the beam while it is commonly not applicable in real structures. Also the effects of shear deformation and rotary inertia were not taken into account. Although Classical Euler–Bernoulli beam theory was used successfully for isotropic beams but since it neglects shear deformation effects, it gives unreliable results for advanced materials, e.g. composites and functionally graded materials (FGMs).

Motivated by these considerations, the need for investigation of vibration characteristics of the functionally graded thick beams considering the effect of shear deformation and rotary inertia is very much felt. In this study, the vibration characteristics of rotating FG beam is analyzed within the context of Timoshenko beam theory. The material properties are assumed to be graded along the thickness of the beam according to FG power-law distribution. The governing equations are derived and solved by applying the semi-analytical differential transform method. Comparisons with the results from the existing literature are provided for validation in special cases. Numerical results are presented to examine the effect of several beam parameters such as constituent volume fractions, slenderness ratios, rotational speed and hub radius on vibration behavior of the rotating thick FG beam.

2 THEORY AND FORMULATION

2.1. Power-law Functionally Graded Material (P-FGM) Beam

One of the most favorable models for FGMs is the power-law model, in which material properties of FGMs are assumed to vary according to a power law about spatial coordinates. The coordinate system for FGM rotating beam is shown in Fig. 1. The length of the beam is L and thickness is h. The FG beam is attached to periphery of a rigid hub of radius R and the hub rotates about z axis at a constant angular speed Ω. A Cartesian coordinate system O(x, y, z) is defined on the central axis of the beam where the x axis is taken along the central axis, the y-axis in the width direction and the z-axis in the depth direction. The FG beam is assumed to be composed of ceramic and metal and effective material properties (P_f) of the FG beam such as Young's modulus E_f, shear modulus G_f and mass density ρ_f are assumed to vary continuously in the thickness direction (z-axis direction) according to an power function of the volume fractions of the constituents while the Poisson's ratio is assumed to be constant in the thickness direction. According to the rule of mixture, the effective material properties, P, can be expressed as (Şimşek, M., and T. Kocatürk, 2010):

$$P_f = P_c V_c + P_m V_m \tag{1}$$

Where P_m, P_c, V_m and V_c are the material properties and the volume fractions of the metal and the ceramic constituents related by:

$$V_c + V_m = 1 \tag{2a}$$

The volume fraction of the metal constituent of the beam is assumed to be given by:

$$V_c = \left(\frac{z}{h} + \frac{1}{2}\right)^q \tag{2b}$$

Here q is the non-negative variable parameter (power-law exponent) which determines the material distribution through the thickness of the beam. Therefore, from Eqs. (1)–(2), the effective material properties of the FG beam can be expressed as follows:

$$P_f(z) = (P_c - P_m)\left(\frac{z}{h} + \frac{1}{2}\right)^q + P_m \tag{3}$$

According to this distribution, bottom surface (z = -h/2) of functionally graded beam is pure metal, whereas the top surface (z = h/2) is pure ceramics.

2.2. Formulation of FGM Beam Using Timoshenko Beam Theory

In a Cartesian coordinate system, x is the distance of the point from the hub edge parallel to beam length, u0 is the axial displacement due to the centrifugal force, z is the vertical distance of the point from the middle plane, w is the transverse displacement of any point on the neutral axis and ϑ is the rotation due to bending. Displacement field components are considered based on Timoshenko beam theory. Considering Hodges et al. (1981) assumption and neglecting terms which are greater than ε^2 strain-displacement and strain energy simplified relations are calculated as follows:

$$\varepsilon_{xx} = u_0' - z\theta' + \frac{(w')^2}{2} \tag{4}$$

$$\gamma_{xz} = w' - \theta \tag{5}$$

$$\gamma_{xy} = 0 \tag{6}$$

In addition, bending strain energy U_b and shear strain energy U_s are given respectively by:

$$U_b = \iiint_V \frac{E(z)\varepsilon^2}{2}\, dV \tag{7}$$

$$U_s = \iiint_V \frac{G(z)\gamma^2}{2}\, dV \tag{8}$$

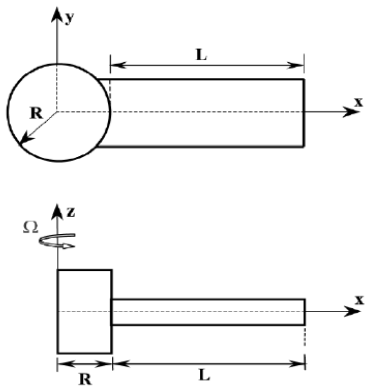

Figure 1: Typical functionally graded beam with Cartesian coordinates.

Substituting equations (4-6) into equations (7-8) leads to

$$U_b = \frac{1}{2}\int_A \int_0^L E(z)\{u_0' - z\theta' + \frac{(w')^2}{2}\}^2 \, dAdx \tag{9}$$

$$U_s = \iiint_V \frac{G(z)(\gamma_{xy}{}^2+\gamma_{xz}{}^2)}{2} \, dV \tag{10}$$

Further, the total strain energy is given by:

$$U = U_s + U_b \tag{11}$$

The axial displacement $u_0'(x)$, which is uniform across the cross section is related to strain $\varepsilon_0(x)$ by:

$$u_0'(x) = \varepsilon_0(x) = \frac{T(x)}{A_1} \tag{12}$$

In which T(x) is centrifugal force and is defined as:

$$T(x) = \int_x^L B_1 \, \Omega^2 (R + x)dx \tag{13}$$

According to equations (9-13) bending and shear strain energy are obtained respectively as follows:

$$U_b = \frac{1}{2}\int_0^L (A_2 \, (\theta')^2 + T(w')^2)dx + const \tag{14}$$

$$U_s = \frac{1}{2}\int_0^L C(w' - \theta)^2 \, dx \tag{15}$$

Here, A_1 and A_2 are bending rigidity and axial rigidity of the beam cross section respectively and are defined as:

$$(A_1, A_2) = \int_{-h/2}^{h/2} E(z)(1, z^2) \, dA \tag{16}$$

And B_1 and C are normal inertia term and shear rigidity factor respectively, which are defined as follows:

$$B_1 = \int_{-h/2}^{h/2} \rho(z)(1, z^2) \, dA \tag{17}$$

$$C = \int kG(z)dA \tag{18}$$

Where A, ρ and E are the area of cross-section, the mass density and modulus of elasticity of the beam respectively and G is the shear modulus and k is the Timoshenko shear correction factor which has been assumed equal to the isotropic case, i.e. k=5/6. Further, substituting equations (14-15) into equation (11) one gets the total strain energy of the beam in the following form:

$$U = \frac{1}{2}\int_0^L A_2(\theta')^2 + T(w')^2 + C(w' - \theta)^2 dx \tag{19}$$

Also the kinetic energy expression is given as:

$$\tau = \frac{1}{2}\int_A \int_0^L (V_x^2 + V_y^2 + V_z^2)\rho \, dA \, dx \tag{20}$$

And the total velocity $\vec{V}$ can be expressed in terms of deformed positions as:

$$\vec{V} = (\dot{x}_1 - \Omega y_1)\vec{i} + (\dot{y}_1 + \Omega y x_1)\vec{j} + \dot{z}_1\vec{k} \tag{21}$$

$$V_x = -\xi\dot{\theta} - \eta\Omega \tag{22}$$

$$V_y = (R + x + u_0 - \xi\theta)\Omega \tag{23}$$

$$V_z = \dot{\omega} \tag{24}$$

Now substituting equations (22-24) into equation (20) kinetic energy is obtained as follows:

$$\tau = \frac{1}{2}\int_0^L [B_1\dot{\omega}^2 + A_2\dot{\theta}^2 + A_2\Omega^2\theta^2]dx \tag{25}$$

2.3. Deriving Governing Equations for Rotating FG Beam

Hamilton's principle is used herein to derive the equations of motion. The principle can be stated in analytical form as:

$$\int_{t_1}^{t_2}(\delta U + \delta V - \delta\tau) = 0 \tag{26}$$

Here, t_1 and t_2 are the initial and end time, respectively; δU is the virtual variation of the strain energy; δV is the virtual variation of the potential energy; and $\delta\tau$ is the virtual variation of the kinetic energy. According to Hamilton's principle, the equations of motion can be obtained as:

$$-B_2\ddot{\theta} + B_2\Omega^2\theta + A_2\theta'' + kC(W' - \theta) = 0 \tag{27}$$

$$-B_1\ddot{W} + (TW')' + kC(W'' - \theta') = 0 \tag{28}$$

Further, the two ends of the Timoshenko cantilever beam (x = 0 and x = L) are subjected to the following boundary conditions:

$$\text{at x=0:} \qquad W(0) = 0\ ,\ \Theta(0) = 0 \tag{29}$$

$$\text{at x=L:} \qquad \Theta'(1) = 0\ ,\ W'(1) - \Theta(1) = 0 \tag{30}$$

Assuming simple harmonic oscillation, w and θ can be written as:

$$W(x,t) = \bar{W}(x)e^{i\omega t} \tag{31}$$

$$\theta(x,t) = \bar{\theta}(x)e^{i\omega t} \tag{32}$$

Substituting equations (31) and (32) into equations (27) and (28), the governing equations are as follows:

$$B_2\ \omega^2\ \bar{\theta}\ + B_2\Omega^2\ \bar{\theta}\ + A_2\bar{\theta}'' + kC(\bar{W}' - \bar{\theta}\ ) = 0 \tag{33}$$

$$B_1\omega^2\bar{W} + (T\bar{W}')' + kC(\bar{W}'' - \bar{\theta}') = 0 \tag{34}$$

The dimensionless parameters which founded according to FGM characteristics are used to simplify the equations and to make comparisons with the studies in literature such as Banerjee (2001) can be given as follows:

$$\eta^2 = \frac{B_1L^4\Omega^2}{A_2},\quad r^2 = \frac{B_2}{A_1L^2}\quad ,\delta = \frac{R}{L}\qquad ,\qquad \xi = \frac{x}{L}$$

$$\mu^2 = \frac{B_1L^4\omega^2}{A_2},\quad s^2 = \frac{A_2}{kCL^2}\ ,\ W(\xi) = \frac{\bar{W}}{L} \tag{35}$$

Then dimensionless expressions for centrifugal force and governing equations are obtained as follows:

$$T(\xi) = B_1\Omega^2L^2\left[\delta(1-\xi) + \frac{(1-\xi^2)}{2}\right] \tag{36}$$

$$\bar{\theta}'' + \eta^2r^2\left(1 + \frac{\omega^2}{\Omega^2}\right)\bar{\theta} + \frac{1}{s^2}(\bar{W}' - \bar{\theta}) = 0 \tag{37a}$$

$$\left\{\left[\delta(1-\xi) + \frac{(1-\xi^2)}{2}\right]\bar{W}'\right\}' + \left(\frac{\omega^2}{\Omega^2}\right)\bar{W} + \frac{1}{s^2\eta^2}(\bar{W}'' - \bar{\theta}') = 0 \tag{37b}$$

Additionally, the dimensionless boundary conditions can be expressed as follows

$$\xi = 0 \qquad \bar{W} = \bar{\theta} = 0 \tag{38a}$$

$$\xi = 1 \qquad \frac{d\bar{W}}{d\xi} - \bar{\theta} = \frac{d\bar{\theta}}{d\xi} = 0 \tag{38b}$$

2.4. Implementation of Differential Transform Method

Generally, it is rather difficult to derive an analytical solution for Eqs. (37-38) due to the nature of non-homogeneity. In this circumstance, the DTM is employed to translate Eqs. (33-34) into a set of ordinary equations. First, the procedure of differential transform method is briefly reviewed. Differential transformation of function y(x) according to Abdel-Halim Hassan (2002) is defined as follows:

$$Y(k) = \frac{1}{k!}\left[\frac{d^k}{dx^k}y(x)\right]_{x=0} \tag{39}$$

In which y(x) is the original function and Y(k) is the transformed function. Besides the differential inverse transformation of Y(k) can be obtained as follows:

$$y(x) = \sum_{n+1}^{\infty} x^k Y(k) \tag{40}$$

Consequently from equations (39-40) we obtain:

$$y(x) = \sum_{k=0}^{\infty} \frac{x^k}{k!}\left[\frac{d^k}{dx^k}y(x)\right]_{x=0} \tag{41}$$

Equation (41) reveals that the concept of the differential transformation is derived from Taylor's series expansion. In real applications the function y(x) in equation (40) can be written in a finite form as:

$$y(x) = \sum_{k=0}^{n} x^k Y(k) \tag{42}$$

In this calculations $y(x) = \sum_{n+1}^{\infty} x^k Y(k)$ is small enough to be neglected, and n is determined by the convergence of the eigenvalues. In Table (1) the basic theorem of DTM is stated while table (2) presents the differential transformation of conventional boundary conditions. Applying the DTM rule on the equations of motion (37) and boundary conditions (38) the next four equations are obtained as:

Original function	Transformed function
$y(x) = \lambda\varphi(x)$	$Y(k) = \lambda\Phi(k)$
$y(x) = \varphi(x) \pm \theta(x)$	$Y(k) = \Phi(k) \pm \Theta(k)$
$y(x) = \frac{d\varphi}{dx}$	$Y(k) = (k+1)\Phi(k+1)$
$y(x) = \frac{d^2\varphi}{dx^2}$	$Y(k) = (k+1)(k+2)\Phi(k+1)$
$y(x) = \varphi(x)\theta(x)$	$Y(k) = \sum_{l=0}^{k} \Phi(l)\Theta(k-l)$
$y(x) = x^m$	$Y(k) = \delta(k-m) = \begin{cases} 1 & k = m \\ 0 & k \neq m \end{cases}$

Table 1: Some of the transformation rules of the one-dimensional DTM.

X=0		X=1	
Original BC	Transformed BC	Original BC	Transformed BC
f(0)=0	F[0]=0	f(1)=0	$\sum_{k=0}^{\infty} F[k] = 0$
$\frac{df}{dx}(0) = 0$	F[1]=0	$\frac{df}{dx}(1) = 0$	$\sum_{k=0}^{\infty} kF[k] = 0$
$\frac{d^2f}{dx^2}(0) = 0$	F[2]=0	$\frac{d^2f}{dx^2}(1) = 0$	$\sum_{k=0}^{\infty} k(k-1)F[k] = 0$
$\frac{d^3f}{dx^3}(0) = 0$	F[3]=0	$\frac{d^3f}{dx^3}(1) = 0$	$\sum_{k=0}^{\infty} k(k-1)(k-2)F[k] = 0$

Table 2: Transformed boundary conditions (B.C.) based on DTM.

$$\left(\delta + 0.5 + \frac{1}{s^2\eta^2}\right)(k+1)(k+2)W(k+2) - \delta(k+1)^2W(k+1) + \left(\frac{\omega^2}{\Omega^2} - \frac{k(k+1)}{2}\right)W(k) - \frac{1}{s^2\eta^2}(k+1)\theta(k+1) = 0 \tag{43}$$

$$(k+1)(k+2)\theta(k+2) + \left[\eta^2 r^2\left(1 + \frac{\omega^2}{\Omega^2}\right) - \frac{1}{s^2}\right]\theta(k) + \frac{1}{s^2}(k+1)W(k+1) = 0 \tag{44}$$

$$\sum_{i=0}^{n} k * \Theta(k) = 0 \tag{45}$$

$$\sum_{i=0}^{n} k * w(k) - \Theta(k) = 0 \tag{46}$$

Here, W(k) and $\vartheta(k)$ are the differential transforms of $w(\xi)$ and $\vartheta(\xi)$, respectively. Substituting W(k) and $\vartheta(k)$ in eqs. (45-46) we have:

$$M_{j1}^{(n)}c_1 + M_{j2}^{(n)}c_2 = 0\,, j = 1,2,3,\dots,n \tag{47}$$

In which M_{ij} are polynomials in terms of ω corresponding to nth term. The matrix form of equation (47) can be prescribed as:

$$\begin{bmatrix} M_{11}^{(n)} & M_{12}^{(n)} \\ M_{21}^{(n)} & M_{22}^{(n)} \end{bmatrix} \begin{Bmatrix} c_1 \\ c_2 \end{Bmatrix} = 0 \tag{48}$$

Further, studying the existence condition of the non-trivial solutions yields the following characteristic equation:

$$\begin{vmatrix} M_{11}^{(n)} & M_{12}^{(n)} \\ M_{21}^{(n)} & M_{22}^{(n)} \end{vmatrix} = 0 \tag{49}$$

Solving equation (49), the i^{th} estimated eigenvalue for nth iteration ($\omega = \omega_i^{(n)}$) may be obtained and the total number of iterations is related to the accuracy of calculations which can be determined by the following equation:

$$\left|\omega_i^{(n)} - \omega_i^{(n-1)}\right| < \varepsilon \tag{50}$$

In this study ε=0.0001 considered in procedure of finding eigenvalues which results in 4 digit precision in estimated eigenvalues. Further a Matlab program has been developed according to DTM rule stated above, in order to find eigenvalues and plot mode shapes.

3 RESULTS AND DISCUSSION

In the present section a numerical testing of the procedure as well as parametric studies are performed in order to establish the validity and usefulness of the DTM approach and the influence of different beam parameters such as constituent volume fractions, slenderness ratios, rotational speed and hub radius on the natural frequencies and mode shapes of the rotating beam is examined. The material properties of the power-law FG constituents are presented in Tables 3 and 4. Relations described in equation (51) are performed in order to calculate the non-dimensional natural frequencies.

$$\lambda = \frac{\omega L^2}{h}\sqrt{\frac{\rho_m}{E_m}} \tag{51}$$

Figures 2-4 show the convergence study of DTM method for first three frequencies. It is found that in DTM method after a certain number of iterations eigenvalues converged to a value with good precision, so the number of iterations is important in DTM method convergence. This fact is obvious in Figures 2 and 3. As seen in Figure 4, third natural frequency converged after 37 iterations with 4 digit precision while according to figure 2 the first natural frequency converged after 33 iterations.

properties	unit	aluminum	Alumina(Al2O3)
E	GPa	70	380
ρ	Kg/m^3	2702	3960
ν	-	0.3	0.3

Table 3: material properties of the FGM constituents (Simsek, 2010).

properties	unit	aluminum	alumina (Al2O3)
E	GPa	70	380
ρ	Kg/m^3	2700	3800
ν	-	0.23	0.23

Table 4: material properties of the FGM constituents (Sina et al., 2009).

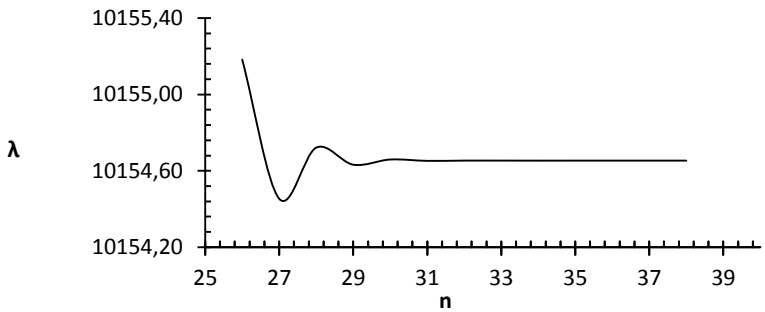

Figure 2: Convergence study for the first frequency of rotating FG beam, q=0, η=8.

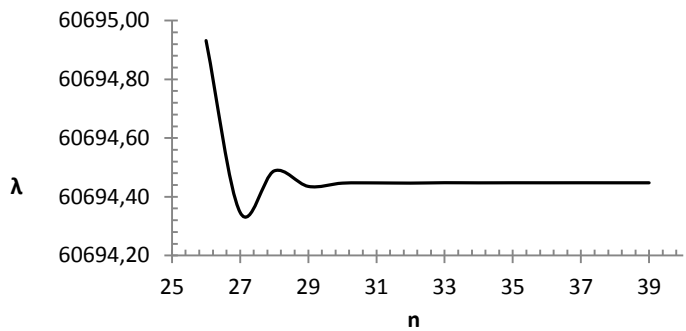

Figure 3: Convergence study for the second frequency of rotating FG beam, q=0, η=8.

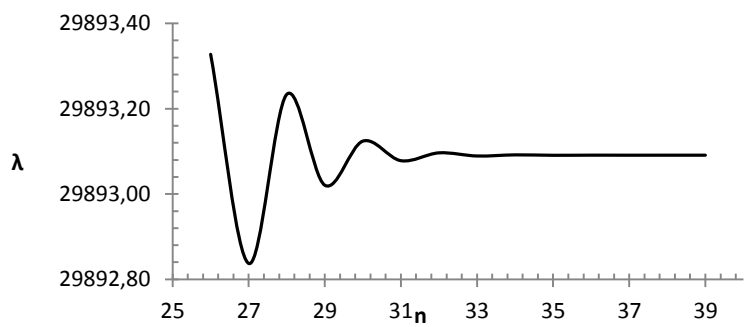

Figure 4: Convergence study for the third frequency of rotating FG beam, q=0, η=8.

	L/h =10	L/h =30	L/h =100
Sina et al.(2009)	0.9960	1.0030	1.0030
Present	0.9858	0.9922	0.9930
% Difference	1.0346	1.0884	1.0070

Table 5: Comparison of fundamental frequencies of FG rotating beams for different L/h ratios.

q	Present	Simsek (2010)	% Difference
ceramic	1.9495	1.9496	0.00359
0.2	1.8286	1.8145	0.7711
0.5	1.7214	1.66046	3.5413
10	1.3555	1.26495	6.6802
metal	1.0198	1.01297	0.6697

Table 6: Comparison of fundamental frequencies of FG rotating beams for different constituent volume fraction exponent.

After looking into the satisfactory results for the convergence of frequencies, one may compare the nondimensional frequencies of FG beam associated with different slenderness ratios and constituent volume fraction exponents. To demonstrate the correctness of present study the results for FG rotating beam are compared with the results of FG rotating beams presented by Simsek (2010) and Sina et al. (2009). Table 5 compares the results of the present study and the results presented by Simsek (2010) which has been obtained by using Lagrange's equations for FG rotating beam with different slenderness ratios while Table 6 compares the presented results with ones by Sina et al. (2009) which has been obtained using an analytical method for various constituent volume fraction exponents. One may clearly notice here that the fundamental frequency parameters obtained in the present investigation are in approximately close enough to the results provided in these literatures that are used for comparison and validates the proposed method of solution.

Frequency parameters of power-law FG beam affected by various parameters are studied in Tables 7-9. Inspection of these tables also reveals that an increase in the value of the power-law exponent leads to a decrease in the fundamental frequencies. The highest frequency values are obtained for full ceramic beam (q = 0) while the lowest frequency values are obtained for full metal beam (q $\rightarrow \infty$). This is due to the fact that, an increase in the value of the power-law exponent results in a decrease in the value of elasticity modulus and the value of bending rigidity. In other words, the beam becomes flexible as the power law exponent increases. Therefore, as also known from mechanical vibrations, natural frequencies decrease as the stiffness of a structure decreases. It is also interesting to note that the decrease in the frequency values due to the increase in the power-law exponent is almost the same for higher mode frequencies.

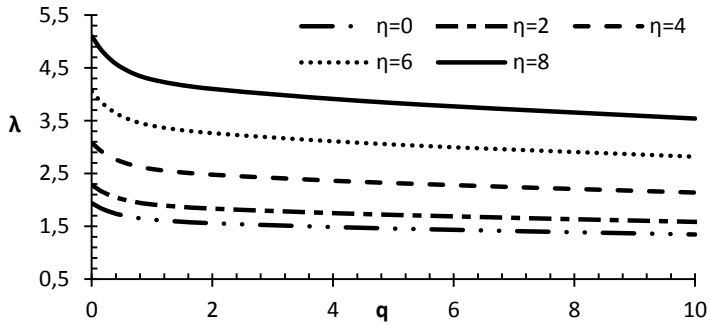

Figure 5: The effect of power-law exponent (q<10) on first natural frequency with different rotational speed parameters, L/h=10.

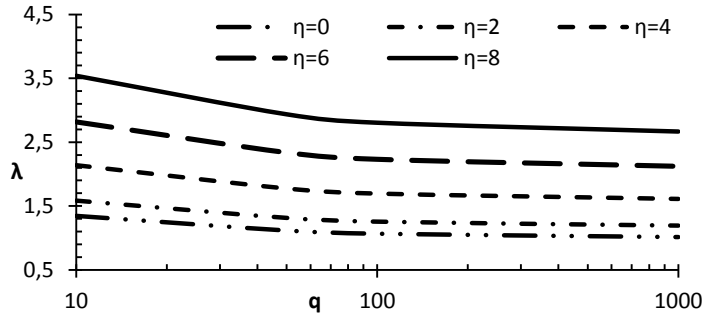

Figure 6: The effect of power-law exponent (q>10) on first natural frequency with different rotational speed parameters, L/h=10.

Also, note that the power-law exponent plays an important role on the fundamental frequency of the FG beam. The effect of power-law exponent on first natural frequency of the FG rotating beam with different rotational speed parameters has been illustrated in Figures 5 and 6 for two cases of q<10 and q>10 respectively.

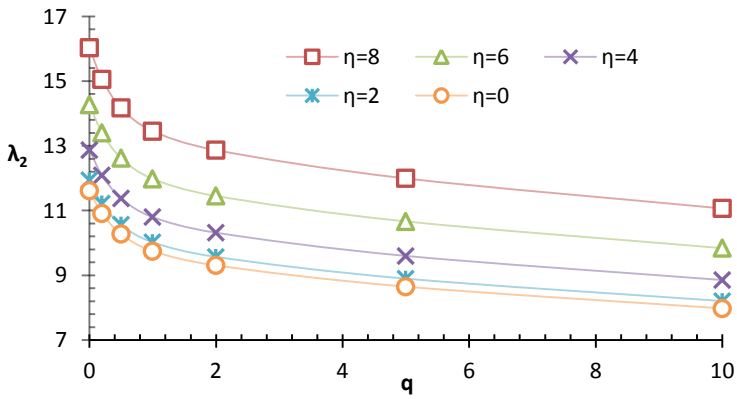

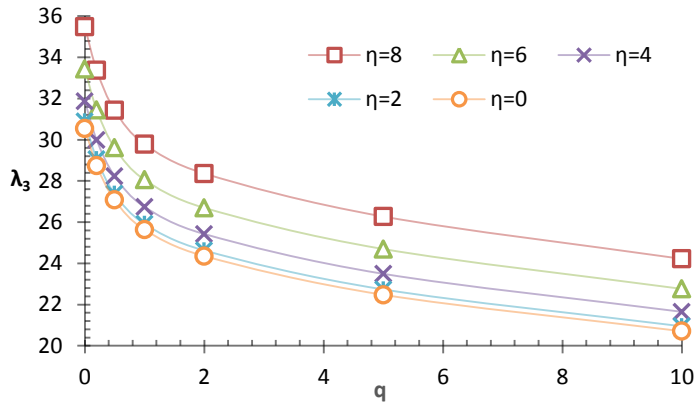

Figure 8: The effect of power-law exponent on third natural frequency with different rotational speed parameters, L/h=10.

It is observed that an increase in the value of the power-law exponent leads to a decrease in the fundamental frequencies. Besides the nonlinear diminishing occurs in frequency when q increased from 0 to 2 and the linear reduction occurs when q is increased from 2 to 10 as shown in Figure 5. Also the effect of the power-law exponent on the second and third mode frequencies of the FG rotating beams is depicted in Figures 7 and 8 respectively. It is showed that the decrease in frequency parameters due to the increase in power-law exponent is also correct for higher mode frequencies. Also the effect of slenderness ratio (L/h) on first natural frequency in different power-law exponents are presented in Table 7 and plotted in Figure 9. As would be expected, the frequencies are increased when the value of L/h is increased and this effect become less significant in higher slenderness ratios. Also the effect of slenderness ratio on first three natural frequencies of FG rotating beam is plotted in Figure 10. It can be concluded that by increasing the L/h ratio the natural frequency parameters increase while the slenderness ratio has more effects on third natural frequency compared with the first and second modes. Figure 9 shows the variation of the fundamental frequency of FG rotating beam with L/h ratio and the power-law exponent, while Figure 10 demonstrates the effect of slenderness ratio of FG rotating beam on its first three natural frequencies. In fact, these figures can be regarded as the visual representation of Table 7. It is noteworthy that, the effect of slenderness ratio on the frequencies is negligible for long FG beams (i.e., $L/h \geqslant 20$); in other words the fundamental frequency of the FG rotating beam is saturated after the value of $L/h = 20$.

q	mode	L/h = 5	L/h=10	L/h=20	L/h =30	L/h =50	L/h=100
0	λ1	4.9877	5.098	5.1312	5.1377	5.1410	5.1424
	λ2	14.6826	16.0314	16.4938	16.5877	16.6369	16.6578
	λ3	29.8114	35.4915	38.0107	38.5744	38.8779	39.0092
0.2	λ1	4.6815	4.7829	4.8132	4.8191	4.8222	4.8235
	λ2	13.8066	15.0516	15.475	15.5607	15.6056	15.6247
	λ3	28.0963	33.3684	35.6797	36.1944	36.4711	36.5907
0.5	λ1	4.4077	4.5028	4.5312	4.5367	4.5396	4.5408
	λ2	13.0029	14.1718	14.5688	14.6491	14.6911	14.709
	λ3	26.4718	31.4259	33.593	34.0752	34.3344	34.4464
1	λ1	4.1853	4.2779	4.3057	4.3111	4.3139	4.3151
	λ2	12.4432	13.4523	13.8403	13.9191	13.9603	13.978
	λ3	25.0154	29.7817	31.8956	32.3686	32.6233	32.7335
2	λ1	4.0066	4.1008	4.1296	4.1353	4.1382	4.1395
	λ2	11.7309	12.8662	13.2655	13.3473	13.3902	13.4086
	λ3	23.6558	28.3609	30.525	31.0167	31.2827	31.3980
5	λ1	3.7400	3.8348	3.8648	3.8707	3.8738	3.8751
	λ2	10.8707	11.9929	12.4027	12.4877	12.5325	12.5517
	λ3	21.7191	26.2714	28.476	28.9882	29.2671	29.3884
10	λ1	3/4514	3.5396	3.5676	3.5731	3.5760	3.5772
	λ2	10.0238	11.0652	11.4476	11.5270	11.5689	11.5868
	λ3	20.003	24.2188	26.2751	26.7543	27.0154	27.129
50	λ1	2.8686	2.9364	2.9573	2.9614	2.9635	2.9644
	λ2	8.3948	9.2106	9.4988	9.5579	9.5889	9.6022
	λ3	16.9114	20.2897	21.8525	22.2084	22.4011	22.4846
100	λ1	2.7417	2.8047	2.8239	2.8277	2.8296	2.8304
	λ2	8.0442	8.8073	9.0734	9.1277	9.1562	9.1684
	λ3	16.2600	19.4438	20.8899	21.2166	21.3931	21.4696
metal	λ1	2.6086	2.6666	2.6840	2.6874	2.6892	2.6899
	λ2	7.6763	8.3841	8.6272	8.6766	8.7024	8.7135
	λ3	15.5780	18.5555	19.8796	20.1762	20.3359	20.4051

Table 7: Variation of the first three natural frequencies of FG rotating beam with L/h ratio for various values of the power-law exponent, η =8.

The other important parameter in vibration behavior of rotating FG beam is its rotational speed parameter. Table 8 presents the variation of first three natural frequencies of FG rotating beam for different rotational speed parameters (η =0, 2, 4, 6, 8) with different power-law exponents.
According to Table 8, increasing the rotational speed increases the first three natural frequencies and as seen in Figure 11 ascending pattern is more sensitive for the first natural frequency. For instance for FG beam with power-law exponent defined as q=2, increasing normal rotational speed from 2 to 4 (100% increase), leads to 35%, 7.8%, 3.2% increase in first three natural frequencies respectively.

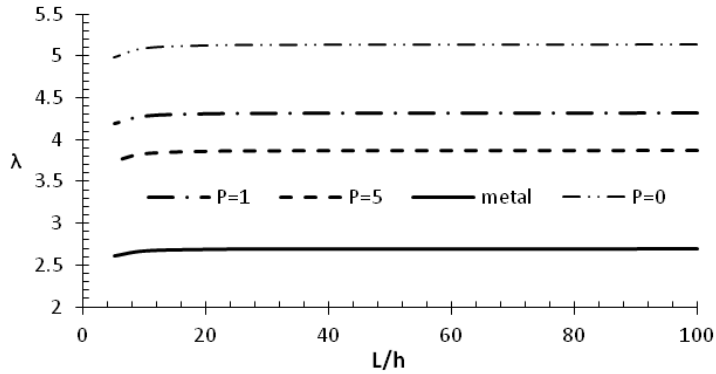

Figure 9: Variation of the fundamental frequency of FG rotating beam with L/h ratio for various power-law exponent.

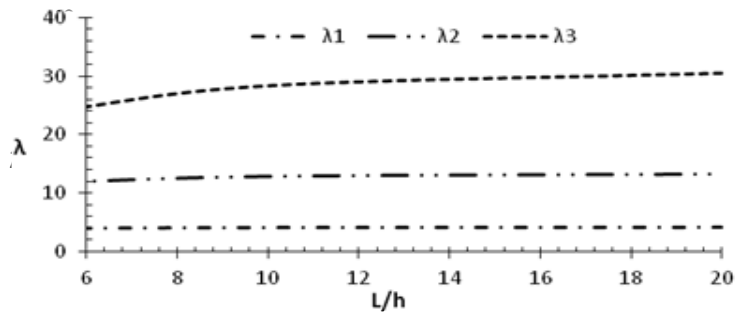

Figure 10: Variation of the first three natural frequencies of FG rotating beam with L/h ratio, q=2 ،η=2

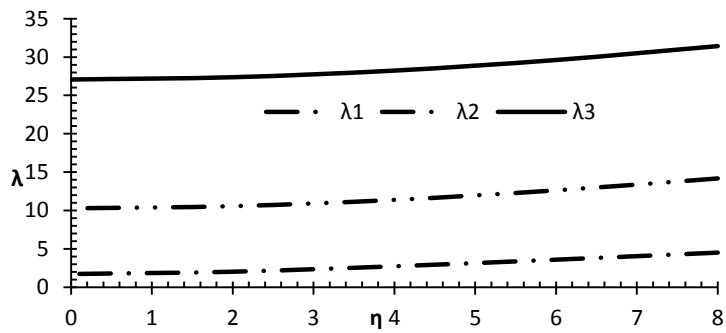

Figure 11: The effect of rotational speed on first three natural frequencies, L/h=10, q=0.5.

The next set of results was obtained to demonstrate the effect of hub radius parameter on the non-dimensional natural frequencies of the rotating FG beam. Variation of the first three natural frequencies of rotating FG beam with various hub radius parameters is tabulated in Table 9. Figure 12 illustrates this effect for first three natural frequencies when L/h =10 ،η=2 and q=0. It is observed that the non-dimensional natural frequencies increase with the hub radius parameter as expected because of the increase in centrifugal stiffening of the beam.

q	mode	η=0	η=2	η=4	η=6	η=8
0	λ1	1.9381	2.2815	3.0801	4.0570	5.0980
	λ2	11.6155	11.9408	12.8669	14.2743	16.0314
	λ3	30.5505	30.8865	31.8701	33.4349	35.4915
0.2	λ1	1.8183	2.1405	2.8896	3.8061	4.7829
	λ2	10.9114	11.2163	12.0844	13.4039	15.0516
	λ3	28.7438	29.0582	29.9784	31.4429	33.3684
0.5	λ1	1.7118	2.0151	2.7204	3.5832	4.5028
	λ2	10.2747	10.5617	11.3787	12.6208	14.1718
	λ3	27.0743	27.3701	28.236	29.6140	31.4259
1	λ1	1.6263	1.9145	2.5846	3.4043	4.2779
	λ2	9.7468	10.0198	10.7969	11.9779	13.4523
	λ3	25.6356	25.9176	26.7429	28.0559	29.7817
2	λ1	1.5589	1.8353	2.4779	3.2636	4.1008
	λ2	9.3053	9.5680	10.3153	11.4502	12.8662
	λ3	24.3533	24.6263	25.4249	26.6944	28.3609
5	λ1	1.4577	1.7165	2.3176	3.1245	3.8348
	λ2	8.6492	8.8962	9.5987	10.6646	11.9929
	λ3	22.474	22.7334	23.4913	24.6945	26.2714
10	λ1	1.3454	1.5843	2.1392	2.8173	3.5396
	λ2	7.9766	8.2049	8.8539	9.8384	11.0652
	λ3	20.7062	20.9461	21.6475	22.7605	24.2188
50	λ1	1.1162	1.3142	1.7744	2.3370	2.9364
	λ2	6.6589	6.8472	7.3828	8.1960	9.2106
	λ3	17.4142	17.6101	18.1832	19.0941	20.2897
100	λ1	1.0662	1.2552	1.6947	2.2321	2.8047
	λ2	6.3735	6.5530	7.0636	7.8393	8.8073
	λ3	16.7097	17.5121	17.4405	18.3065	19.4438
Metal	λ1	1.0137	1.1934	1.6111	2.1220	2.6666
	λ2	6.0738	6.2442	6.7286	7.4649	8.3841
	λ3	15.9694	16.1453	16.6601	17.4791	18.5555

Table 8: The effect of rotational speed parameter on natural frequencies of FG rotating beam with different power law exponent for the case: L/h=10.

Another set of results was obtained to illustrate some representative mode shapes of the rotating FG beam. Figure 13 shows the first normalized mode shape of the rotating FG beam plotted for different values of L/d (5, 20). The second and the third normalized mode shapes are plotted in Figures 14 and 15. Seeing as the material properties are constant through the beam axis, no change occurs in mode shapes and their profiles as presented in Figures 13-15.

mode	δ=0	δ=0.02	δ=0.04	δ=0.06	δ=0.08	δ=0.1	δ=0.12
λ_1	2.2815	2.2899	2.2983	2.3066	2.3149	2.3231	2.3314
λ_2	11.9408	11.9495	11.9581	11.9667	11.9753	11.9839	11.9925
λ_3	30.8865	30.896	30.9054	30.9149	30.9243	30.9338	30.9432

Table 9: The effect of hub radius parameter on the first three natural frequencies, L/h =10 ،η_j=2 ، q=0.

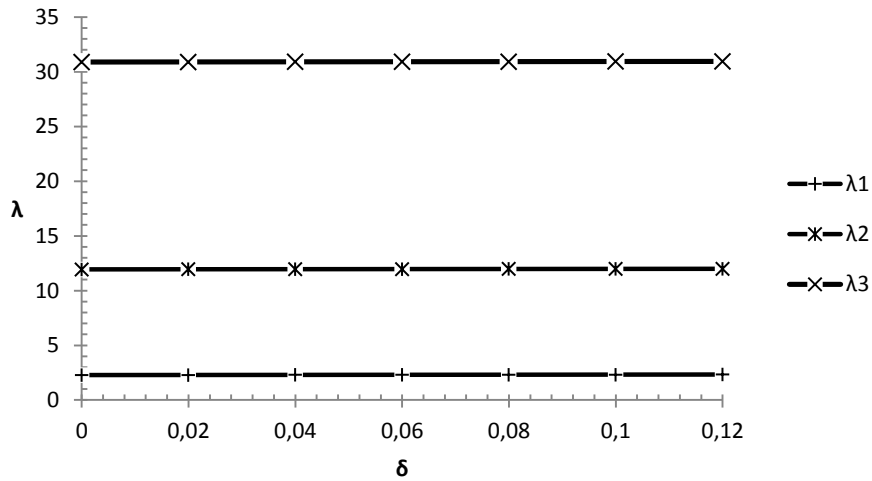

Figure 12: Effect of hub radius parameter on first three natural frequencies, L/h =10 ،η_j=2 ، q=0.

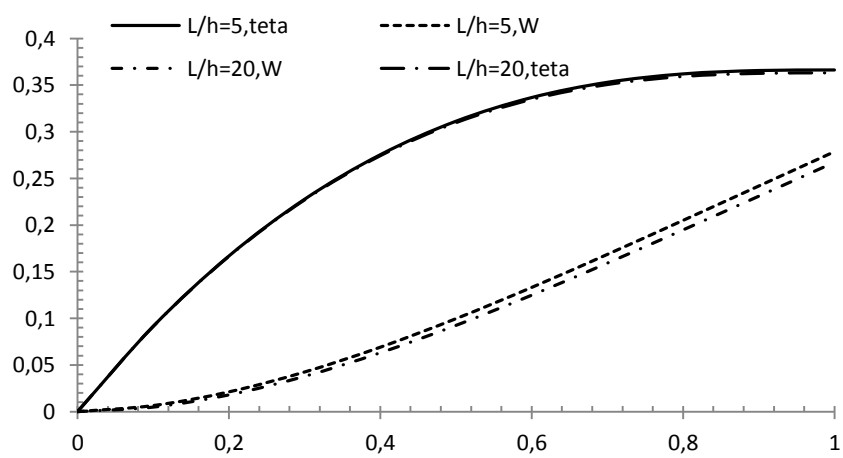

Figure 13: The normalized first mode shape of rotating FG beam for different slenderness ratios.

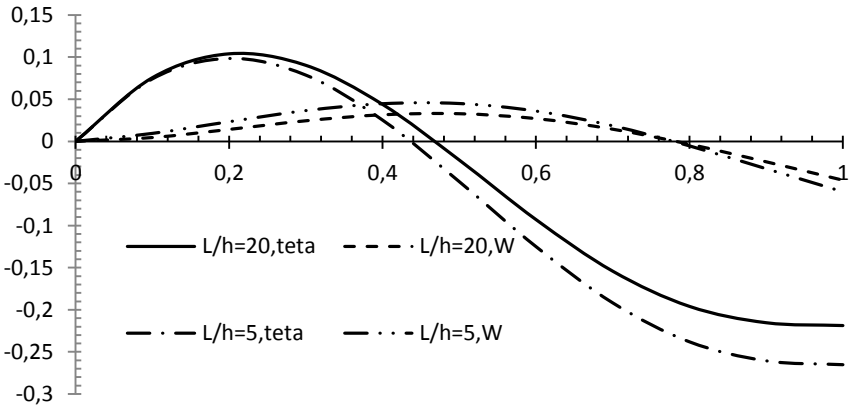

Figure 14: The normalized second mode shape of rotating FG beam for different slenderness ratios.

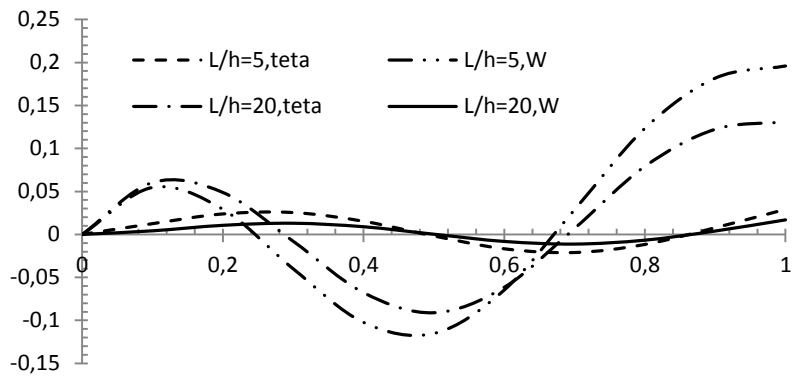

Figure 15: The normalized third mode shape of rotating FG beam for different slenderness ratios.

4 CONCLUSIONS

In this paper a new model to study the vibration characteristics of rotating beams made of functionally graded materials has been introduced using semi analytical differential transform method. The model has been deduced employing a formulation accounting for shear-deformability relationships. Results of the presented work are compared and validated with available results in literature. Effect of different parameters includes constituent volume fractions, slenderness ratios, rotational speed and hub radius on the natural frequencies and mode shapes of the rotating beam is investigated. The DTM method is an accurate and uncomplicated numerical method to solve eigenvalue problems. The presented expressions are convenient and efficient for the analysis of the FG beams and they are valid for a wide range of vibration amplitudes. The FG beam is analyzed for Power-law model, changing power-law exponent leads to different distributions of metal and ceramic in FG beam. It is concluded that by increasing power-law exponent decreases the frequency parameters while increasing the slenderness ratios resulted in increasing the frequency parameters; this effect becomes less significant when the value become larger. Rotational speed has a considerable effect on

natural frequency parameter, variation of this parameter have a direct relation with frequency parameter. In comparison with other parameters hub radius has not a sensitive effect on natural frequency, increasing hub radius increases natural frequency with low gradient.

References

Abdel-Halim Hassan, I. H. "On solving some eigenvalue problems by using a differential transformation." Applied Mathematics and Computation 127.1 (2002): 1-22.

Aydogdu, Metin, and Vedat Taskin. "Free vibration analysis of functionally graded beams with simply supported edges." Materials & design 28.5 (2007): 1651-1656.

Banerjee, J. R. "Dynamic stiffness formulation and free vibration analysis of centrifugally stiffened Timoshenko beams." Journal of Sound and Vibration 247.1 (2001): 97-115.

Ebrahimi, F. "Analytical investigation on vibrations and dynamic response of functionally graded plate integrated with piezoelectric layers in thermal environment." Mechanics of Advanced Materials and Structures 20.10 (2013): 854-870.

Ebrahimi, F., and A. Rastgoo. "Free vibration analysis of smart annular FGM plates integrated with piezoelectric layers." Smart Materials and Structures 17.1 (2008a): 015044.

Ebrahimi, F, and A. Rastgoo. "An analytical study on the free vibration of smart circular thin FGM plate based on classical plate theory." Thin-Walled Structures 46.12 (2008b): 1402-1408.

Ebrahimi, F., A. Rastgoo, and A. A. Atai. "A theoretical analysis of smart moderately thick shear deformable annular functionally graded plate." European Journal of Mechanics-A/Solids 28.5 (2009a): 962-973.

Ebrahimi, F., Naei, M.H. and Abbas Rastgoo. "Geometrically nonlinear vibration analysis of piezoelectrically actuated FGM plate with an initial large deformation." Journal of mechanical science and technology 23.8 (2009b): 2107-2124.

Ho, Shing Huei, and Cha'O. Kuang Chen. "Free transverse vibration of an axially loaded non-uniform spinning twisted Timoshenko beam using differential transform." International journal of mechanical sciences 48.11 (2006): 1323-1331.

Hodges, Dewey Yang, and Michael Yang Rutkowski. "Free-vibration analysis of rotating beams by a variable-order finite-element method." AIAA Journal 19.11 (1981): 1459-1466.

Kapuria S, Bhattacharyya M, Kumar AN. Bending and free Vibration response of layered functionally graded beams, a theoretical model and its experimental validation. "Composite Structures", 82(3), (2008): 390-402.

Ke, Liao-Liang, Jie Yang, and Sritawat Kitipornchai. "An analytical study on the nonlinear vibration of functionally graded beams." Meccanica 45.6 (2010): 743-752.

Li, X-F., Y-A. Kang and J-X. Wu. "Exact frequency equations of free vibration of exponentially functionally graded beams." Applied Acoustics 74.3 (2013): 413-420.

Mei, C. "Application of differential transformation technique to free vibration analysis of a centrifugally stiffened beam." Computers & Structures 86.11 (2008): 1280-1284.

Mohanty, S. C., R. R. Dash, and T. Rout. "Free Vibration of a Functionally Graded Rotating Timoshenko Beam Using FEM." Advances in Structural Engineering 16.2 (2013): 405-418.

Pradhan, K. K., and S. Chakraverty. "Free vibration of Euler and Timoshenko functionally graded beams by Rayleigh–Ritz method." Composites Part B: Engineering 51 (2013): 175-184.

Shahba, A., Attarnejad R., and Zarrinzadeh H. "Free Vibration Analysis of Centrifugally Stiffened Tapered Functionally Graded Beams."Mechanics of Advanced Materials and Structures." 20.5 (2013): 331-338.

Şimşek, M., "Fundamental frequency analysis of functionally graded beams by using different higher-order beam theories." Nuclear Engineering and Design 240 (2010): 697-705.

Sina, S. A., H. M. Navazi, and H. Haddadpour. "An analytical method for free vibration analysis of functionally graded beams." Materials & Design 30.3 (2009): 741-747.

Zhou, J. K. "Differential transformation and its applications for electrical circuits." (1986): 1279-1289.